Proceedings of the
44th IEEE Conference on Decision and Control, and
the European Control Conference 2005
Seville, Spain, December 12-15, 2005

Cross-track control for underactuated autonomous vehicles

Even Børhaug and Kristin Y. Pettersen
Dept. of Eng. Cybernetics, Norwegian University of Science and Technology, NO-7491, Trondheim, Norway.
Even.Borhaug@itk.ntnu.no and Kristin.Y.Pettersen@itk.ntnu.no

Abstract— **This paper considers 3-dimensional cross-track control for a class of underactuated autonomous vehicles. A control strategy is presented that guarantees global κ-exponential stability of the cross-track error to straight line trajectories in three dimensional space. The results are based on a Line-of-Sight guidance algorithm and stability results are proven using nonlinear cascaded systems theory. Globally κ-exponentially stabilizing controllers are synthesized using the technique of sliding mode with eigenvalue decomposition, and the performance of the proposed control strategy is evaluated by a case study with an AUV.**

I. INTRODUCTION

The route of an autonomous vehicle can compactly be described in terms of way-points, with the reference trajectory made up of the straight lines interconnecting the way-points. A way-point is usually a fixed point in space, given in Cartesian coordinates in some inertial reference frame. The way-point description leads to a attractive decoupling between the geometric task of controlling the position and orientation of the autonomous vehicle and the dynamic task of controlling the speed of the vehicle ([1]). The way-points can be decided without having to specify the desired speed profile of the vehicle, and the speed profile can then be changed without having to recompute the way-points. This would not have been the case if the reference trajectory was given in terms of a time-dependent trajectory. In this paper we exploit this feature and use a Line-of-Sight (LOS) guidance law to achieve stability to the reference trajectory while the desired forward speed of the vehicle can be controlled to any nonzero value.

Guidance algorithms based on the LOS principle was initially developed for controlling the flight path of missiles, but similar ideas was soon adopted for path control of other mechanical systems. LOS algorithms are commonly used for way-point tracking and cross-track control. When the objective is to converge a set of way-points in the order they are given, the problem is referred to as way-point tracking and when the distance to the reference trajectory, the cross-track error, is to be controlled, the control problem is referred to as cross-track control.

Over the last decade, way-point tracking and cross-track control for marine surface vessels, autonomous underwater vehicles and wheeled mobile robots have been studied by numerous authors. Way-point tracking and cross-track control of underactuated marine surface vessels are studied in [2] and [3]. Both papers utilize the LOS guidance principle and controllers are designed to give the closed loop system a cascaded structure. Stability is investigated and global asymptotic stability and global κ-exponential stability of the heading and cross-track error is proven.

LOS-based control of underactuated surface vessels are also studied in [4] and [5]. In both papers, controllers that globally asymptotically stabilizes the heading and surge speed of the vessel are presented, but stability of the cross-track error is not addressed.

[6] and [7] considers planar and 3D path following for underactuated autonomous underwater vehicles respectively. In both papers, the path tracking problem is described in the Serret Frenet coordinate frame and nonlinear control strategies are proposed that guarantees global asymptotic convergence to the reference path. The planar path following problem is also considered in [8]. Assuming no knowledge of the curvature of the desired path, a nonlinear control strategy that guarantees boundedness of the tracking error is proposed.

[9] presents results on planar way-point tracking for autonomous underwater vehicles. A controller is synthesized using integrator backstepping and asymptotic convergence to the desired way-point is proven. Multivariable sliding mode control of low-speed autonomous underwater vehicles is studied in [10]. Controllers for steering, diving and speed are designed based on decoupled models and a LOS guidance algorithm is used for path following.

Underactuation of mechanical systems often leads to non-holonomic constraints on the acceleration of the system. As pointed out in the famous paper by Brockett [11], a large class of underactuated systems cannot be stabilized by a continuously differentiable, time-invariant state feedback control law, even if they are strongly accessible. This fact prevents the control strategy presented in this paper, which gives a time-invariant state feedback controller, from holding at zero forward speed. However, in this paper we assume that the forward speed is non-zero and address the underactuated (straight) *path following problem* and not the nonholonomic *stabilization* problem. Some results on stabilization of non-holonomic systems in general are given in [12] and [13], and for mobile robots in particular in [14], [15] and [16].

The purpose of this paper is to develop a control strategy that guarantees global κ-exponential stability to straight-line trajectories in three dimensional space, for a class of underactuated autonomous vehicles. We seek to incorporate the nice features of line of sight guidance, a guidance method that is much used in practice, while also guaranteeing stability of the cross-track error. Finally, the purpose is also to show how nonlinear cascaded systems theory can be used

0-7803-9568-9/05/$20.00 ©2005 IEEE

to achieve a separation property, where the stability of the overall system is not explicitly dependent on a particular controller, but rather on the dynamical properties of the closed loop system. This makes the obtained results more general and easier extendable to other systems and other controllers.

The outline of this paper is as follows: In Section II some preliminaries are presented. In Section III the vehicle model is presented and the control objective is defined. Section IV presents the main stability results and Section V presents a suitable controller based on the sliding mode principle. Simulation results for the proposed control strategy applied to an AUV is presented in Section VI.

II. Preliminaries

Definition 1 (Global κ-exponential stability [17]). *The system*

$$\dot{\boldsymbol{x}} = \boldsymbol{f}(t,\boldsymbol{x}) \ \ , \ \boldsymbol{f}(t,\boldsymbol{0}) = \boldsymbol{0} \ \forall \ t \geq t_0 \ , \ \ \boldsymbol{x} \in \boldsymbol{R}^n$$

is globally κ-exponentially stable if there exists a class $\mathcal{K}$ function $\kappa(\cdot)$ and a constant $\gamma > 0$ such that $\forall \boldsymbol{x}(t_0) \in \boldsymbol{R}^n$

$$||\boldsymbol{x}(t)|| \leq \kappa(||\boldsymbol{x}(t_0)||)e^{-\gamma(t-t_0)} \qquad \forall t \geq t_0 \geq 0$$

Result 1. *Global κ-exponential stability is equivalent to global uniform asymptotic stability (GUAS) plus local uniform exponential stability (LUES) ([18]).*

III. The system model and control objective

We consider 3-dimensional cross-track control for a class of underactuated mechanical systems; underactuated autonomous vehicles, with independent control in surge, pitch and yaw. In particular, we assume that the roll motion of the vehicle can be neglected and that the dynamics of the vehicle can be described by the 5-DOF model:

$$\dot{\boldsymbol{\eta}} = \boldsymbol{J}(\boldsymbol{\eta})\boldsymbol{\nu} \quad \text{(1a)}$$

$$\boldsymbol{M}\dot{\boldsymbol{\nu}} + \boldsymbol{C}(\boldsymbol{\nu})\boldsymbol{\nu} + (\boldsymbol{D} + \boldsymbol{D}(\boldsymbol{\nu}))\boldsymbol{\nu} + \boldsymbol{g}(\boldsymbol{\eta}) = \boldsymbol{B}_\tau\boldsymbol{\tau} \quad \text{(1b)}$$

where $\boldsymbol{\eta} \in \boldsymbol{R}^5$, $\boldsymbol{\nu} \in \boldsymbol{R}^5$ and $\boldsymbol{\tau} \in \boldsymbol{R}^3$ are given by

$$\boldsymbol{\eta} = (x \ y \ z \ \theta \ \psi)^T \quad \boldsymbol{\nu} = (u \ v \ w \ q \ r)^T \quad \boldsymbol{\tau} = (\tau_1 \ \tau_2 \ \tau_3)^T$$

Here, (x, y, z) is the inertial position, θ is the pitch angle and ψ is the yaw angle. Furthermore, u is the surge velocity, v is the sway velocity, w is the heave velocity, q is the pitch rate and r is the yaw rate. Finally, τ_1, τ_2 and τ_3 are independent control inputs.

Moreover, $\boldsymbol{J}(\boldsymbol{\eta})$ is the kinematic transformation matrix, $\boldsymbol{M}$ is the mass and inertia matrix, $\boldsymbol{C}(\boldsymbol{\nu})$ is the Coriolis and centripetal matrix, $\boldsymbol{D}$ and $\boldsymbol{D}(\boldsymbol{\nu})$ are damping and friction matrices, $\boldsymbol{g}(\boldsymbol{\eta})$ accounts for gravity and buoyancy and $\boldsymbol{B}_\tau$ is the actuator configuration matrix, where rank $(\boldsymbol{B}_\tau) = 3$. The mass and inertia matrix is assumed to be constant, symmetric and positive definite, such that:

$$\dot{\boldsymbol{M}} = \boldsymbol{0} \quad \text{and} \quad \boldsymbol{x}^T\boldsymbol{M}\boldsymbol{x} = \boldsymbol{x}^T\boldsymbol{M}^T\boldsymbol{x} > 0 \ \ \forall \boldsymbol{x} \in \boldsymbol{R}^5\backslash\{\boldsymbol{0}\}$$

The differential kinematics (1a) relates the body fixed velocities $\boldsymbol{\nu}$ to the inertial velocities $\dot{\boldsymbol{\eta}}$. In particular, the differential kinematics are given by ([19]):

$$\dot{x} = \cos\psi\cos\theta u - \sin\psi v + \cos\psi\sin\theta w \quad (2)$$

$$\dot{y} = \sin\psi\cos\theta u + \cos\psi v + \sin\theta\sin\psi w \quad (3)$$

$$\dot{z} = -\sin\theta u + \cos\theta w \quad (4)$$

$$\dot{\theta} = q \quad (5)$$

$$\dot{\psi} = \frac{1}{\cos\theta}r \quad (6)$$

We place the origin of the inertial reference coordinate system in the previous way-point with the z-axis pointing down and the x-axis pointing towards the next way-point. The y-axis is chosen to complete the right-handed coordinate system. With this choice of reference coordinate system, the y-position of the vehicle equals the horizontal cross track error, the z-position equals the vertical cross-track error and the x-axis corresponds to the desired straight-line trajectory. The control objective is to force the autonomous vehicle to track the straight-line trajectory interconnecting two consecutive way-points, while maintaining a desired non-zero, constant forward speed. In particular, if we define

$$\tilde{\boldsymbol{\eta}} \triangleq \begin{pmatrix} 0 & y & z & \theta & \psi \end{pmatrix} \quad \tilde{\boldsymbol{\nu}} \triangleq \begin{pmatrix} \tilde{u} & v & w & q & r \end{pmatrix}$$

where the surge speed error $\tilde{u}$ is defined as

$$\tilde{u} \triangleq u - u_d \quad (7)$$

the control objective is to find a smooth, time-invariant state feedback control law $\boldsymbol{\tau} = \boldsymbol{\tau}(\tilde{\boldsymbol{\eta}}, \tilde{\boldsymbol{\nu}})$ that makes the origin $(\tilde{\boldsymbol{\eta}}, \tilde{\boldsymbol{\nu}}) = (\boldsymbol{0}, \boldsymbol{0})$ globally κ-exponentially stable.

Remark: Note that by controlling the surge speed u, we are not interested in controlling the x-position as a function of time. Therefore, we impose no control objective on x.

IV. Global κ-exponential cross-track maneuvering

In this section we consider the cross-track error dynamics and apply a LOS guidance algorithm. Using nonlinear cascaded systems theory, we prove global κ-exponential stability of the cross-track errors y and z, provided that the surge speed error dynamics and the LOS angle tracking error dynamics are made globally κ-exponentially stable.

We pick a point that lies a constant distance $\Delta > 0$ ahead of the vehicle, along the trajectory. The line of sight is the line joining the vehicle and the selected point. The angles formed by the xy-plane projection and the xz-plane projection of the line of sight and the x-axis of the reference coordinate system, is referred to as the LOS angles. The constant Δ is referred to as the look-ahead distance. With reference to Figure 1, the LOS angles are given by the following two expressions:

$$\theta_{LOS} = \tan^{-1}(\frac{z}{\Delta}) \quad (8)$$

$$\psi_{LOS} = \tan^{-1}(\frac{-y}{\Delta}) \quad (9)$$

Note that, we have used the same Δ in both (8) and (9),

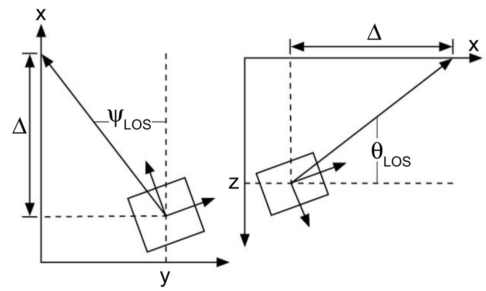

Fig. 1. Illustration of LOS angles ψ_{LOS} and θ_{LOS}.

but they could generally be different. We choose the LOS angles and their derivatives as reference input for the control system, i.e.

$$\theta_d = \theta_{LOS} \tag{10}$$

$$\psi_d = \psi_{LOS} \tag{11}$$

$$q_d = \dot{\theta}_{LOS} = \frac{\Delta}{\Delta^2 + z^2}\dot{z} \tag{12}$$

$$r_d = \dot{\psi}_{LOS}\cos\theta = \cos\theta\frac{\Delta}{\Delta^2 + y^2}\dot{y} \tag{13}$$

Furthermore, we define the tracking errors in pitch and yaw, and the tracking errors in pitch and yaw rate as

$$\tilde{\theta} \triangleq \theta - \theta_d \quad \tilde{\psi} \triangleq \psi - \psi_d \quad \tilde{q} \triangleq q - q_d \quad \tilde{r} \triangleq r - r_d \tag{14}$$

Applying definitions (7) and (14), (3-4) can be written

$$\begin{aligned}\dot{y} &= \sin(\tilde{\psi} + \psi_d)\cos(\tilde{\theta} + \theta_d)(\tilde{u} + u_d)\\ &\quad + \cos(\tilde{\psi} + \psi_d)v + \sin(\tilde{\theta} + \theta_d)\sin(\tilde{\psi} + \psi_d)w \end{aligned}\tag{15}$$

$$\dot{z} = -\sin(\tilde{\theta} + \theta_d)(\tilde{u} + u_d) + \cos(\tilde{\theta} + \theta_d)w \tag{16}$$

By expanding the trigonometric functions of sums of angles and factoring the result with respect to the tracking errors, (15-16) can be written

$$\begin{aligned}\dot{y} &= \sin\psi_d\cos\theta_d u_d + \cos\psi_d v\\ &\quad + \sin\theta_d\sin\psi_d w + \boldsymbol{\chi}^T\tilde{\boldsymbol{x}}\end{aligned}\tag{17}$$

$$\dot{z} = -\sin\theta_d u_d + \cos\theta_d w + \boldsymbol{\omega}^T\tilde{\boldsymbol{x}} \tag{18}$$

where $\tilde{\boldsymbol{x}} \triangleq (\tilde{u} \;\; \tilde{\theta} \;\; \tilde{\psi})^T$, $\boldsymbol{\chi}^T \triangleq (\chi_1 \;\; \chi_2 \;\; \chi_3)^T$ and $\boldsymbol{\omega}^T \triangleq (\omega_1 \;\; \omega_2 \;\; \omega_3)^T$. The individual components of the vectors $\boldsymbol{\chi}$ and $\boldsymbol{\omega}$ are given by

$$\begin{aligned}
\chi_1 &= \sin(\tilde{\psi} + \psi_d)\cos(\tilde{\theta} + \theta_d)\\
\chi_2 &= \frac{\sin\tilde{\theta}}{\tilde{\theta}}\Big(-\sin\theta_d\cos\tilde{\psi}\sin\psi_d u_d\\
&\qquad + \cos\theta_d\sin(\tilde{\psi} + \psi_d)w\Big)\\
&\quad + \frac{\cos\tilde{\theta} - 1}{\tilde{\theta}}\Big(\cos\tilde{\psi}\sin\psi_d\cos\theta_d u_d\\
&\qquad + \sin\theta_d\cos\tilde{\psi}\sin\psi_d w\Big)\\
\chi_3 &= \frac{\sin\tilde{\psi}}{\tilde{\psi}}\Big(\cos\psi_d\cos(\tilde{\theta} + \theta_d)u_d\\
&\qquad - \sin\psi_d v + \cos\tilde{\theta}\sin\theta_d\cos\psi_d w\Big)\\
&\quad + \frac{\cos\tilde{\psi} - 1}{\tilde{\psi}}(\sin\psi_d\cos\theta_d u_d + \cos\psi_d v\\
&\qquad + \sin\theta_d\sin\psi_d w)\\
\omega_1 &= -\sin(\tilde{\theta} + \theta_d)\\
\omega_2 &= -\frac{\sin\tilde{\theta}}{\tilde{\theta}}(\cos\theta_d u_d + \sin\theta_d w)\\
&\qquad + \frac{1 - \cos\tilde{\theta}}{\tilde{\theta}}(\sin\theta_d u_d - \cos\theta_d w)\\
\omega_3 &= 0
\end{aligned}$$

Note that $\lim_{x\to 0}\frac{\sin x}{x} = 1$ and $\lim_{x\to 0}\frac{\cos x - 1}{x} = 0$, such that $\boldsymbol{\chi}$ and $\boldsymbol{\omega}$ are well-defined.

Inserting (8) and (9) into (17) and (18), yields

$$\begin{aligned}\dot{y} &= -\frac{y}{\sqrt{y^2+\Delta^2}}\frac{\Delta}{\sqrt{z^2+\Delta^2}}u_d + \frac{\Delta}{\sqrt{y^2+\Delta^2}}v\\ &\quad - \frac{yz}{\sqrt{y^2+\Delta^2}\sqrt{z^2+\Delta^2}}w + \boldsymbol{\chi}^T\tilde{\boldsymbol{x}}\end{aligned}\tag{19}$$

$$\dot{z} = -\frac{z}{\sqrt{z^2+\Delta^2}}u_d + \frac{\Delta}{\sqrt{z^2+\Delta^2}}w + \boldsymbol{\omega}^T\tilde{\boldsymbol{x}} \tag{20}$$

With a slight abuse of notation, suppose there exists controllers such that the two closed loop systems

$$\dot{\boldsymbol{\xi}} = \boldsymbol{f}_\xi(t, \boldsymbol{\xi}) \tag{21}$$

$$\dot{\boldsymbol{\zeta}} = \boldsymbol{f}_\zeta(t, \boldsymbol{\zeta}) \tag{22}$$

where

$$\boldsymbol{\xi} \triangleq \begin{pmatrix}\tilde{\boldsymbol{x}}^T & \tilde{q} & \tilde{r} & v & w\end{pmatrix}^T \quad \boldsymbol{\zeta} \triangleq \begin{pmatrix}\tilde{u} & \tilde{\theta} & \tilde{q} & w\end{pmatrix}^T$$

are globally κ-exponentially stable. We can then state the following two propositions.

Proposition 1. *Let $u_d > 0$ be the constant desired surge speed. If $\boldsymbol{\zeta} = \mathbf{0}$ is made a globally κ-exponentially stable equilibrium point of (22), then $(z, \boldsymbol{\zeta}) = (0, \mathbf{0})$ is a globally κ-exponentially stable equilibrium point of (20) and (22).*

Proof. The system (20) and (22) can be seen as a cascaded system:

$$\dot{z} = -\frac{z}{\sqrt{z^2+\Delta^2}}u_d + \boldsymbol{h}_z(t, z, \boldsymbol{\omega})\boldsymbol{\zeta} \tag{23a}$$

$$\dot{\boldsymbol{\zeta}} = \boldsymbol{f}_\zeta(t, \boldsymbol{\zeta}) \tag{23b}$$

where

$$\boldsymbol{h}_z(t, z, \boldsymbol{\omega}) = \begin{pmatrix}\omega_1 & \omega_2 & 0 & \frac{\Delta}{\sqrt{z^2+\Delta^2}}\end{pmatrix}$$

where ω_1 and ω_2 are elements of the vector $\boldsymbol{\omega}$. Note that $\omega_3 = 0$, hence (23a) is independent of both $\tilde{\psi}$, $\tilde{r}$ and y. The cascaded system (23) can be seen as the nominal system

$$\Sigma_1 : \quad \dot{z} = -\frac{u_d}{\sqrt{z^2+\Delta^2}}z$$

perturbed by the output of the globally κ-exponentially stable system

$$\Sigma_2: \quad \dot{\boldsymbol{\zeta}} = \boldsymbol{f}_\zeta(t, \boldsymbol{\zeta})$$

through the interconnection term $\boldsymbol{h}_z(t, z, \boldsymbol{\omega})$.

To prove global κ-exponential stability of the origin $(z, \boldsymbol{\zeta}) = (0, \mathbf{0})$ of (23), we apply two results from the theory of cascaded nonlinear systems. We first prove that the nominal Σ_1 system is globally κ-exponentially stable. We choose the positive definite and radially unbounded Lyapunov Function Candidate (LFC) $V = \frac{1}{2}z^2$ and differentiate V along the solution of Σ_1:

$$\dot{V} = -\frac{u_d}{\sqrt{z^2 + \Delta^2}} z^2 < 0$$

Since V is radially unbounded and $\dot{V}$ is negative definite along the trajectories of Σ_1, it follows that the origin $z = 0$ is a GUAS equilibrium of the nominal system Σ_1.

Moreover, on the ball $D = \{z \in \boldsymbol{R} \mid |z| \leq r\}$, $r > 0$, we have that

$$\dot{V} \leq -\frac{u_d}{\sqrt{r^2 + \Delta^2}} z^2 \leq -k_z z^2 < 0$$

for some $0 < k_z \leq \frac{u_d}{\sqrt{r^2+\Delta^2}}$, and it follows from ([20], Th. 4.10) that the origin $z = 0$ is a LUES equilibrium of the nominal system Σ_1. By Result 1, $z = 0$ is also a globally κ-exponentially stable equilibrium of the nominal system Σ_1.

In order to prove that the origin $(z, \boldsymbol{\zeta}) = (0, \mathbf{0})$ of the cascaded system (23) is also globally κ-exponentially stable, we apply ([15], Th. 7) and ([15], Lemma 8). We start by verifying the three assumptions of ([15], Th. 7). The first assumption, the GUAS assumption on the nominal system, was proven above. The third assumption, the integral assumption on the perturbing signal, is satisfied trivially by the assumption that Σ_2 is globally κ-exponentially stable. However, it remains to show that the second assumption, the assumption on the interconnection, is satisfied. That is the linear growth condition

$$||\boldsymbol{h}_z(t, z, \boldsymbol{\omega})|| \leq \theta_1(||\boldsymbol{\zeta}||) + \theta_2(||\boldsymbol{\zeta}||)|z|$$

where $\theta_1, \theta_2 : \boldsymbol{R}^+ \to \boldsymbol{R}^+$ are continuous functions. Writing out $||\boldsymbol{h}_z(t, z, \boldsymbol{\omega})||_1$ yields

$$\begin{aligned} ||\boldsymbol{h}_z(t, z, \boldsymbol{\omega})||_1 &= |\omega_1| + |\omega_2| + \left|\frac{\Delta}{\sqrt{z^2 + \Delta^2}}\right| \\ &\leq 2(1 + |u_d| + |w|) \\ &\leq 2(1 + c + ||\boldsymbol{\zeta}||_1) \end{aligned}$$

where $|u_d| \leq c$. Hence the assumption on the interconnection is satisfied with $\theta_1 = 2(1+c+||\boldsymbol{\zeta}||)$ and $\theta_2 = 0$, and by ([15], Th. 7), the origin $(z, \boldsymbol{\zeta}) = (\mathbf{0}, \mathbf{0})$ of the cascaded system (23) is GUAS. Moreover, since Σ_1 and Σ_2 are both globally κ-exponentially stable it follows from ([15], Lemma 8) that the origin $(z, \boldsymbol{\zeta}) = (0, \mathbf{0})$ of the cascaded system (23) is globally κ-exponentially stable. □

Proposition 2. *Let $u_d > 0$ be the constant desired surge speed. If $\boldsymbol{\xi} = \mathbf{0}$ is made a globally κ-exponentially stable equilibrium point of (21), then $(y, z, \boldsymbol{\xi}) = (0, 0, \mathbf{0})$ is a globally κ-exponentially stable equilibrium point of (19-20) and (21).*

Proof. The systems (19) and (21) can be seen as a cascaded system:

$$\dot{y} = -\frac{u_d}{\sqrt{y^2 + \Delta^2}} \frac{\Delta}{\sqrt{z^2 + \Delta^2}} y + \boldsymbol{h}_y(t, y, z, \boldsymbol{\chi})\boldsymbol{\xi} \tag{24a}$$

$$\dot{\boldsymbol{\xi}} = \boldsymbol{f}_\xi(t, \boldsymbol{\xi}) \tag{24b}$$

where

$$\boldsymbol{h}_y(t, y, z, \boldsymbol{\chi}) = \left(\boldsymbol{\chi}^T \; g_{y2} \; g_{y3} \; g_{y4} \; g_{y5}\right)$$

$$g_{y2} = 0 \quad g_{y4} = \frac{\Delta}{\sqrt{y^2+\Delta^2}}$$

$$g_{y3} = 0 \quad g_{y5} = \frac{-yz}{\sqrt{y^2+\Delta^2}\sqrt{z^2+\Delta^2}}$$

We proceed as in the proof of Proposition 1 and show that the origin of the nominal system

$$\Sigma_1: \; \dot{y} = -\frac{u_d}{\sqrt{y^2 + \Delta^2}} \frac{\Delta}{\sqrt{z^2 + \Delta^2}} y$$

is globally κ-exponentially stable. It should be noted that the nominal system Σ_1 is non-autonomous, since it depends on the time-varying signal $z(t)$. However, since $\boldsymbol{\zeta}$, used in the proof of Proposition 1, is a subvector of $\boldsymbol{\xi}$ and the additional elements of $\boldsymbol{\xi}$ do not affect the $\dot{z}$-equation, the stability property of $z = 0$ is invariant when perturbed by $\boldsymbol{\xi}$ in place of $\boldsymbol{\zeta}$. This follows from the proof of Proposition 1 by replacing $\boldsymbol{\zeta}$ with $\boldsymbol{\xi}$ and extending the interconnection term $\boldsymbol{h}_z$ with corresponding zeros. The rest of the proof is then the same and since $\boldsymbol{\xi} = \mathbf{0}$ is a globally κ-exponentially stable equilibrium point of (21) and $u_d > 0$ by assumption, global κ-exponential stability of $(z, \boldsymbol{\xi}) = (0, \mathbf{0})$ follows. The two propositions could easily be combined into one result. We have split it in two to clearly illustrate which variables that have to converge in order for the horizontal and vertical cross-track errors to converge, respectively. We think this gives a more general understanding of why and when the LOS algorithm works.

From the global κ-exponential stability property of $(z, \boldsymbol{\xi}) = (0, \mathbf{0})$, there exists an upper bound on the position variable $z(t)$. In particular, there exists a $b_z = b_z(z_0) > 0$, independent of t_0, such that $|z(t)| \leq b_z$, $\forall t \geq t_0$. We take the positive definite and radially unbounded LFC $V_2 = \frac{1}{2}y^2$ and differentiate V_2 along the solution of Σ_1:

$$\dot{V}_2 = -\frac{u_d}{\sqrt{y^2 + \Delta^2}} \frac{\Delta}{\sqrt{b_z^2 + \Delta^2}} y^2 < 0$$

Since $V_2 > 0$ and radially unbounded and $\dot{V}_2$ is negative definite along the trajectories of Σ_1, $y = 0$ is a GUAS equilibrium point of the nominal system Σ_1. Moreover, for $y \in D_y = \{y \in \boldsymbol{R} \mid |y| \leq r\}$, $r > 0$, $\dot{V}_2$ satisfies

$$\dot{V}_2 = -\frac{u_d}{\sqrt{r^2 + \Delta^2}} \frac{\Delta}{\sqrt{b_z^2 + \Delta^2}} y^2 \leq -k_y y^2 < 0$$

where

$$0 < k_y \leq \frac{u_d}{\sqrt{r^2 + \Delta^2}} \frac{\Delta}{\sqrt{b_z^2 + \Delta^2}}$$

That is, for $y \in D_y$ $\dot{V}_2$ is upper bounded by a quadratic and negative definite function, and by ([20], Th. 4.10), $y = 0$ is a LUES equilibrium point of the nominal system Σ_1. By Result 1, $y = 0$ is also a globally κ-exponentially stable equilibrium point of the nominal system Σ_1.

The perturbing system

$$\Sigma_2 : \ \dot{\boldsymbol{\xi}} = \boldsymbol{f}_{\xi}(t, \boldsymbol{\xi}, \boldsymbol{\eta}, \boldsymbol{\nu})$$

is globally κ-exponentially stable by assumption. To show that the origin $(y, \boldsymbol{\xi}) = (0, \boldsymbol{0})$ of the cascaded system (24) is globally κ-exponentially stable, we once more apply ([15], Th. 7) and ([15], Lemma 8). Again the first and third assumption of ([15], Th. 7) are trivially satisfied. Moreover, the second assumption is also satisfied, as can be seen by writing out the 1-norm of $\boldsymbol{h}_y(t, y, z, \boldsymbol{\chi})$:

$$\begin{aligned} ||\boldsymbol{h}_y(t, y, z, \boldsymbol{\chi})||_1 &\leq ||\boldsymbol{\chi}||_1 + \left| \frac{\Delta}{\sqrt{y^2 + \Delta^2}} \right| \\ &\quad + \left| \frac{-yz}{\sqrt{y^2 + \Delta^2}\sqrt{z^2 + \Delta^2}} \right| \\ &\leq 3 + 4(|u_d| + |w|) + 2|v| \\ &\leq 3 + 4c + 6||\boldsymbol{\xi}||_1 \end{aligned}$$

where $|u_d| < c$. Thus the second assumption is satisfied with $\theta_1 = 3 + 4c + 6||\boldsymbol{\xi}||_1$ and $\theta_2 = 0$, and by ([15], Th. 7) the origin $(y, \boldsymbol{\xi}) = (0, \boldsymbol{0})$ of the cascaded system (24) is GUAS. Furthermore, since Σ_1 and Σ_2 are both globally κ-exponentially stable, it follows from ([15], Lemma 8) that $(y, \boldsymbol{\xi}) = (0, \boldsymbol{0})$ is globally κ-exponentially stable. $\square$

V. Controller Design

In the preceding section, we presented two propositions giving sufficient conditions for global κ-exponential stability of the cross-track errors y and z. In particular, it was shown that a controller rendering $(\tilde{u}, \tilde{\theta}, \tilde{q}, w) = (0, 0, 0, 0)$ globally κ-exponentially stable, with $u_d > 0$ and θ_d chosen according to (10), was sufficient to guarantee global κ-exponential stability of the vertical cross-track error z. It was further shown that global κ-exponential stability of the extended origin $(\tilde{\boldsymbol{x}}, \tilde{q}, \tilde{r}, v, w) = (\boldsymbol{0}, 0, 0, 0, 0)$, with $u_d > 0$ and θ_d and ψ_d chosen according to (10) and (11), was sufficient to guarantee global κ-exponential stability of both the vertical and horizontal cross-track error. In this section, we design controllers using *sliding mode with eigenvalue decomposition* that guarantees that the closed loop system satisfies the conditions of Proposition 1 and 2.

We write (1b) in the following form

$$\dot{\boldsymbol{\nu}} = \boldsymbol{A}\boldsymbol{\nu} + \boldsymbol{B}\boldsymbol{\tau} + \boldsymbol{f}(\boldsymbol{\nu}, \boldsymbol{\eta}) \tag{25}$$

where

$$\boldsymbol{A} = \boldsymbol{M}^{-1}\boldsymbol{D} \qquad \boldsymbol{B} = \boldsymbol{M}^{-1}\boldsymbol{B}_{\tau}$$
$$\boldsymbol{f}(\boldsymbol{\nu}, \boldsymbol{\eta}) = \boldsymbol{M}^{-1}(-\boldsymbol{C}(\boldsymbol{\nu})\boldsymbol{\nu} - \boldsymbol{D}(\boldsymbol{\nu})\boldsymbol{\nu} - \boldsymbol{g}(\boldsymbol{\eta}))$$

We split the system into two subsystems by defining

$$\begin{aligned} \boldsymbol{\nu}_1 &= (u \ w \ q)^T & \boldsymbol{u}_1 &= (\tau_1 \ \tau_2)^T \\ \boldsymbol{\nu}_2 &= (v \ r)^T & u_2 &= \tau_3 \end{aligned}$$

This decomposition results in the following two state space models

$$\dot{\boldsymbol{\nu}}_1 = \boldsymbol{A}_1\boldsymbol{\nu}_1 + \boldsymbol{B}_1\boldsymbol{u}_1 + \boldsymbol{f}_1(\boldsymbol{\nu}, \boldsymbol{\eta}) \tag{26}$$
$$\dot{\boldsymbol{\nu}}_2 = \boldsymbol{A}_2\boldsymbol{\nu}_2 + \boldsymbol{b}_2 u_2 + \boldsymbol{f}_2(\boldsymbol{\nu}, \boldsymbol{\eta}) \tag{27}$$

where $\boldsymbol{f}_1$ and $\boldsymbol{f}_2$ also accounts for the interaction between the subsystems.

A. Surge Force and Pitch Torque Control

We extend (26) by adding the pitch angle dynamics (5) and introduce integral action in the surge mode by defining a new augmented state

$$\boldsymbol{x}_1 \triangleq \begin{pmatrix} \int_{t_0}^{t} u(s)ds & \boldsymbol{\nu}_1^T & \theta \end{pmatrix}^T$$

and the corresponding desired state

$$\boldsymbol{x}_{1d} \triangleq \begin{pmatrix} \int_{t_0}^{t} u_d(s)ds & u_d & 0 & q_d & \theta_d \end{pmatrix}^T$$

The integral action gives increased robustness to modeling errors and environmental disturbances.

We define the tracking error

$$\bar{\boldsymbol{x}}_1 \triangleq \boldsymbol{x}_1 - \boldsymbol{x}_{1d}$$

and compute the corresponding tracking error dynamics:

$$\dot{\bar{\boldsymbol{x}}}_1 = \bar{\boldsymbol{A}}_1\boldsymbol{x}_1 + \bar{\boldsymbol{B}}_1\boldsymbol{u}_1 + \bar{\boldsymbol{f}}_1(\boldsymbol{\nu}, \boldsymbol{\eta}) - \dot{\boldsymbol{x}}_{1d} \tag{28}$$

where

$$\bar{\boldsymbol{A}}_1 = \begin{pmatrix} 0 & 1 & 0 & 0 & 0 \\ 0 & a_{11} & a_{12} & a_{13} & 0 \\ 0 & a_{21} & a_{22} & a_{23} & 0 \\ 0 & a_{31} & a_{32} & a_{33} & 0 \\ 0 & 0 & 0 & 1 & 0 \end{pmatrix}$$

$$\bar{\boldsymbol{B}}_1 = \begin{pmatrix} 0 & 0 \\ b_{11} & b_{12} \\ b_{21} & b_{22} \\ b_{31} & b_{32} \\ 0 & 0 \end{pmatrix} \quad \bar{\boldsymbol{f}}_1(\boldsymbol{\nu}, \boldsymbol{\eta}) = \begin{pmatrix} 0 \\ \boldsymbol{f}_1(\boldsymbol{\nu}, \boldsymbol{\eta}) \\ 0 \end{pmatrix}$$

Here, a_{ij} is the element of row i and column j of $\boldsymbol{A}_1$ and b_{ij} is the element of row i and column j of $\boldsymbol{B}_1$.

To partially stabilize the system (28), we choose the state feedback controller:

$$\boldsymbol{u}_1 = -\bar{\boldsymbol{K}}_1(\boldsymbol{x}_1 - \boldsymbol{x}_{1d}) + \boldsymbol{u}_{10} \tag{29}$$

Here $\boldsymbol{u}_{10}$ is an auxiliary control input and $\bar{\boldsymbol{K}}_1 = (\boldsymbol{K}_1 \ \boldsymbol{0}_{2\times 1})$ is chosen by pole placement such that the upper left 4×4 submatrix of $\boldsymbol{A}_{1c} \triangleq \bar{\boldsymbol{A}}_1 - \bar{\boldsymbol{B}}_1\bar{\boldsymbol{K}}_1$ is Hurwitz. Note that the linear state feedback leaves the pitch angle uncontrolled. Inserting (29) into (28) gives the closed-loop tracking error dynamics:

$$\dot{\bar{\boldsymbol{x}}}_1 = \boldsymbol{A}_{1c}\boldsymbol{x}_1 + \bar{\boldsymbol{B}}_1\bar{\boldsymbol{K}}_1\boldsymbol{x}_{1d} + \bar{\boldsymbol{B}}_1\boldsymbol{u}_{10} + \bar{\boldsymbol{f}}_1(\boldsymbol{\nu}, \boldsymbol{\eta}) - \dot{\boldsymbol{x}}_{1d} \tag{30}$$

To apply sliding mode design, we define a sliding surface

$$\sigma_1(\bar{\boldsymbol{x}}_1) \triangleq \boldsymbol{h}_1^T\bar{\boldsymbol{x}}_1 \tag{31}$$

where $\boldsymbol{h}_1 \in \boldsymbol{R}^5$ is a constant vector to be determined, and derive the dynamics of the sliding surface by differentiating $\sigma_1(\bar{\boldsymbol{x}}_1)$ along the solutions of (30):

$$\begin{aligned} \dot{\sigma}_1(\bar{\boldsymbol{x}}_1) = \boldsymbol{h}_1^T \big(&\boldsymbol{A}_{1c}\boldsymbol{x}_1 + \bar{\boldsymbol{B}}_1\bar{\boldsymbol{K}}_1\boldsymbol{x}_{1d} + \bar{\boldsymbol{B}}_1\boldsymbol{u}_{10} \\ &+ \bar{\boldsymbol{f}}_1(\boldsymbol{\nu}, \boldsymbol{\eta}) - \dot{\boldsymbol{x}}_{1d}\big) \end{aligned} \tag{32}$$

The idea underlying a sliding mode approach, is to design the control input such that the system trajectories converge to the sliding surface. In this case, we design $\boldsymbol{u}_{10}$ such that the trajectories $\bar{\boldsymbol{x}}(t)$ converge to the sliding surface $\sigma_1(\bar{\boldsymbol{x}}_1) = 0$. We take the positive definite and radially unbounded LFC $V_1 = \frac{1}{2}\sigma_1^2$ and differentiate V_1 along the solutions of (32):

$$\begin{aligned}\dot{V}_1 = \sigma_1 \boldsymbol{h}_1^T \big(&\boldsymbol{A}_{1c}\boldsymbol{x}_1 + \bar{\boldsymbol{B}}_1 \bar{\boldsymbol{K}}_1 \boldsymbol{x}_{1d} + \bar{\boldsymbol{B}}_1 \boldsymbol{u}_{10} \\ &+ \bar{\boldsymbol{f}}_1(\boldsymbol{\nu},\boldsymbol{\eta}) - \dot{\boldsymbol{x}}_{1d}\big)\end{aligned}$$

We assume that $\boldsymbol{h}_1^T \bar{\boldsymbol{B}}_1 \neq \boldsymbol{0}$, such that the system is controllable and choose the control $\boldsymbol{u}_{10}$ according to

$$\begin{aligned}\boldsymbol{u}_{10} = (\boldsymbol{h}_1^T \bar{\boldsymbol{B}}_1)^T (\boldsymbol{h}_1^T \bar{\boldsymbol{B}}_1 \bar{\boldsymbol{B}}_1^T \boldsymbol{h}_1)^{-1} \Big(&- \boldsymbol{h}_1^T \bar{\boldsymbol{A}}_1 \boldsymbol{x}_{1d} \\ &- \boldsymbol{h}_1^T \bar{\boldsymbol{f}}_1(\boldsymbol{\nu},\boldsymbol{\eta}) + \boldsymbol{h}_1^T \dot{\boldsymbol{x}}_d - k_{\sigma_1}\sigma_1 \Big) \quad (33)\end{aligned}$$

where $k_{\sigma_1} > 0$ is an adjustable controller gain. With $\boldsymbol{u}_{10}$ given by (33), the Lyapunov Function derivative $\dot{V}_1$ is given by:

$$\dot{V}_1 = \sigma_1 \bar{\boldsymbol{x}}_1^T \boldsymbol{A}_{1c}^T \boldsymbol{h}_1 - k_{\sigma_1}\sigma_1^2$$

To get rid of the term $\sigma_1 \bar{\boldsymbol{x}}_1^T \boldsymbol{A}_{1c}^T \boldsymbol{h}_1$, we note that $\boldsymbol{A}_{1c}^T$ is square, but singular. The matrix $\bar{\boldsymbol{A}}_1$ is singular, and because the last column of $\bar{\boldsymbol{K}}_1$ is chosen equal to zero, $\bar{\boldsymbol{A}}_c$ is singular. Then $\bar{\boldsymbol{A}}_c^T$ is singular. From linear algebra we know that a singular matrix has one or more zero eigenvalues. Thus choosing $\boldsymbol{h}_1$ as a right eigenvector of $\boldsymbol{A}_{1c}^T$ corresponding to a zero eigenvalue, renders $\bar{\boldsymbol{x}}_1^T \boldsymbol{A}_{1c}^T \boldsymbol{h}_1 = \lambda \bar{\boldsymbol{x}}_1^T \boldsymbol{h}_1$ zero. Continuing the Lyapunov analysis then yields

$$\dot{V}_1 = -k_{\sigma_1}\sigma_1^2 < 0$$

which shows that $\dot{V}_1$ is quadratic and negative definite. Moreover, since $V_1 > 0$ is a quadratic Lyapunov function, V_1 satisfies ([20], Th. 4.10), and $\sigma_1 = 0$ is a GUES equilibrium point of (32). For the proof of the fact that $\sigma_1(\bar{\boldsymbol{x}}_1) = 0 \Rightarrow \bar{\boldsymbol{x}}_1 = \boldsymbol{0}$, we refer to [21] and [22].

B. Yaw Torque Control

We proceed as in the previous section and extend (27) with the yaw-angle dynamics (6) and define a new augmented state and a corresponding desired state:

$$\bar{\boldsymbol{x}}_2 \triangleq \begin{pmatrix} \boldsymbol{\nu}_2^T & \psi \end{pmatrix}^T \qquad \bar{\boldsymbol{x}}_{2d} \triangleq \begin{pmatrix} 0 & r_d & \psi_d \end{pmatrix}^T$$

The resulting state space model is then given by

$$\dot{\bar{\boldsymbol{x}}}_2 = \bar{\boldsymbol{A}}_2 \bar{\boldsymbol{x}}_2 + \bar{\boldsymbol{b}}_2 u_2 + \bar{\boldsymbol{f}}_2(\boldsymbol{\nu},\boldsymbol{\eta})$$

where

$$\bar{\boldsymbol{A}}_2 = \begin{pmatrix} a_{11} & a_{12} & 0 \\ a_{21} & a_{22} & 0 \\ 0 & 1 & 0 \end{pmatrix}, \quad \bar{\boldsymbol{b}}_2 = \begin{pmatrix} b_{11} \\ b_{21} \\ 0 \end{pmatrix}$$

$$\bar{\boldsymbol{f}}_2(\boldsymbol{\nu},\boldsymbol{\eta}) = \begin{pmatrix} 0 \\ \boldsymbol{f}_1(\boldsymbol{\nu},\boldsymbol{\eta}) \\ \frac{1-\cos\theta}{\cos\theta} r \end{pmatrix}$$

Here a_{ij} is the element of row i and column j of $\boldsymbol{A}_2$ and b_{ij} is the element of row i of $\boldsymbol{b}_2$. Again, we define a sliding surface

$$\sigma_2(\bar{\boldsymbol{x}}_2) \triangleq \boldsymbol{h}_2^T \bar{\boldsymbol{x}}_2 \qquad (34)$$

where $\boldsymbol{h}_2 \in \boldsymbol{R}^3$ and $\bar{\boldsymbol{x}}_2 \triangleq \boldsymbol{x}_2 - \boldsymbol{x}_{2d}$. Following the same procedure as for the surge and pitch subsystem, we choose the control law

$$u_2 = -\bar{\boldsymbol{k}}_2^T (\boldsymbol{x}_2 - \boldsymbol{x}_{2d}) + u_{20} \qquad (35)$$

where the auxiliary control input u_{20} is chosen according to

$$u_{20} = \frac{1}{\boldsymbol{h}_2^T \boldsymbol{b}_2}(-\boldsymbol{h}_2^T \bar{\boldsymbol{A}}_2 \boldsymbol{x}_{2d} - \boldsymbol{h}_2^T \bar{\boldsymbol{f}}_2(\boldsymbol{\nu},\boldsymbol{\eta}) + \boldsymbol{h}^T \dot{\boldsymbol{x}}_d - k_{\sigma_2}\sigma_2)$$

where $k_{\sigma_2} > 0$. The vector $\boldsymbol{h}_2$ is chosen as the right eigenvector of $\boldsymbol{A}_{2c}^T = (\bar{\boldsymbol{A}}_2 - \bar{\boldsymbol{b}}_2 \bar{\boldsymbol{k}}_2^T)^T$ corresponding to a zero eigenvalue. Again $\boldsymbol{A}_{2c}^T$ has a zero a zero eigenvalue, since it is a singular matrix. We choose the positive definite and radially unbounded LFC $V_2 = \frac{1}{2}\sigma_2^2$ and differentiate V_2 along the solution of (34):

$$\dot{V}_2 = \sigma_2 \boldsymbol{h}_2^T (\boldsymbol{A}_{2c} \bar{\boldsymbol{x}}_2 - k_{\sigma_2}\sigma) = -k_{\sigma_2}\sigma_2^2 < 0$$

Then, since the Lyapunov Function derivative $\dot{V}_2$ is quadratic and negative definite and $V_2 > 0$ is quadratic, it follows from ([20], Th. 4.10) that $\sigma_2 = 0$ is a GUES equilibrium point of (34).

The surge and pitch controller (29) and the yaw controller (35) renders $(\tilde{u}, w, \tilde{q}, \tilde{\theta}) = (0,0,0,0)$ and $(v, \tilde{r}, \tilde{\psi})$ GUES respectively. Therefore, the combined origin $(\tilde{\boldsymbol{x}}, \tilde{q}, \tilde{r}, v, w) = (\boldsymbol{0}, 0, 0, 0, 0)$ is also GUES. Then, provided that $u_d > 0$ and θ_d, ψ_d, q_d and r_d are chosen according to (10)-(13), all the assumptions of Proposition 1 and 2 are satisfied. We can then conclude that the developed controllers guarantee global κ-exponential stability of both the vertical and the horizontal cross-track error and the desired forward speed of the vehicle.

VI. CASE STUDY: HUGIN AUV

The proposed control strategy was simulated in Matlab/Simulink on a full 6DOF model of the HUGIN AUV. The HUGIN AUV has three available controls: a propeller thrust T and two rudder deflections δ_D and δ_S for diving and steering respectively. The AUV can be described by the 6DOF model

$$\boldsymbol{M}\dot{\boldsymbol{\nu}} + \boldsymbol{C}(\boldsymbol{\nu})\boldsymbol{\nu} + \boldsymbol{D}(\boldsymbol{\nu})\boldsymbol{\nu} + \boldsymbol{g}(\boldsymbol{\eta}) = \boldsymbol{B}_\tau \boldsymbol{\tau} \qquad (36)$$

where $\boldsymbol{\tau} = (T \ \delta_D \ \delta_S)^T$ and the mass and inertia matrix

$$\boldsymbol{M} = \begin{pmatrix} m_{11} & 0 & 0 & 0 & m_{15} & 0 \\ 0 & m_{22} & 0 & -m_{15} & 0 & m_{26} \\ 0 & 0 & m_{33} & 0 & m_{35} & 0 \\ 0 & -m_{15} & 0 & m_{44} & 0 & 0 \\ m_{15} & 0 & m_{35} & 0 & m_{55} & 0 \\ 0 & m_{26} & 0 & 0 & 0 & m_{66} \end{pmatrix}$$

is constant, symmetric and positive definite. The total damping matrix is given by

$$\boldsymbol{D}(\boldsymbol{\nu}) = \begin{pmatrix} d_{11} + d_{1u}|u| & 0 & 0 & 0 & 0 & 0 \\ 0 & d_{22} & 0 & 0 & 0 & d_{26} \\ 0 & 0 & d_{33} & 0 & d_{35} & 0 \\ 0 & 0 & 0 & d_{44} & 0 & 0 \\ 0 & 0 & d_{53} & 0 & d_{55} & 0 \\ 0 & d_{26} & 0 & 0 & 0 & d_{66} \end{pmatrix}$$

and the actuator configuration matrix is given by

$$\boldsymbol{B}_\tau = \begin{pmatrix} 1 & 0 & 0 \\ 0 & Y_{\delta_S} & 0 \\ 0 & 0 & Z_{\delta_D} \\ 0 & 0 & 0 \\ 0 & 0 & Z_{\delta_S} l_x \\ 0 & Y_{\delta_S} l_x & 0 \end{pmatrix}$$

A propeller thrust saturation was included by limiting the propeller revolution corresponding to the propeller thrust to ± 230 RPM. The rudders were saturated at $\pm 20°$ and a rudder slew rate of $\pm 10°$/s was used. The system was given zero initial surge speed and simulated with the following desired speed profile

$$u_d(t) = \begin{cases} 1.25m/s & 0 < t \leq 70 \\ 1.75m/s & 70 < t \leq 110 \\ 1.50m/s & 110 < t \leq 150 \end{cases}$$

The initial cross-track errors were chosen as $y(0) = 50$m and $z(0) = 30$m. The reference signals in pitch and yaw were computed using (8), (9), (12) and (13). To generate smooth derivatives, each reference signal was filtered by a low-pass filter before being fed to the control system. The look-ahead distance was chosen as $\Delta = 20$m. Δ is an important control parameter. For AUV operations it is generally important to have a well-damped motion, as this is important to the sensor data quality. There will always be a trade-off between convergence rate and how well-damped the motion is. A nice feature of the proposed control algorithm is that it is easy to adjust the trade-off between the two concerns by adjusting Δ. Choosing Δ small, leads to a high convergence rate, but will typically lead to overshoot. Choosing Δ large, overcomes the problem of overshoot, but gives a slower convergence rate. The simulation results are shown in figure 2(a)-2(c).

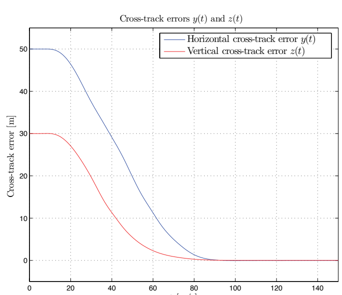

(a) Cross-track errors $y(t)$ and $z(t)$.

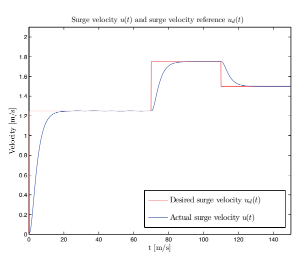

(b) $u(t)$ and $u_d(t)$.

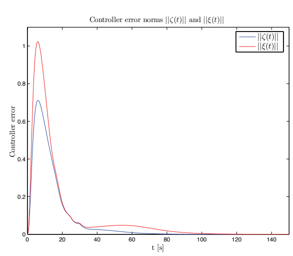

(c) $||\boldsymbol{\zeta}(t)||_2$, $||\boldsymbol{\xi}(t)||_2$.

Fig. 2.

VII. Conclusions

In this paper, a cross-track control scheme for uderactuated autonomous vehicles that guarantees global κ-exponential stability of the cross-track error to straight line trajectories has been presented. In particular, we proposed a control scheme based on a line of sight guidance law and designed stabilizing controllers using sliding mode with eigenvalue decomposition. Stability of the cross-track error was proven using nonlinear cascaded systems theory, and the performance of the proposed control scheme was indicated through a case study with the HUGIN AUV.

References

[1] R. Skjetne, T. Fossen, and P. Kokotivic, "Output maneuvering for a class of nonlinear systems," in *Proc. IFAC World Congress Automatic Control*, Barcelona, Spain, July 2002.

[2] K. Pettersen and E. Lefeber, "Way-point tracking control of ships," in *Proc. of 40th IEEE Conference on Decision and Control*, vol. 1, December 2001, pp. 940–945.

[3] E. Fredriksen and K. Pettersen, "Global κ-exponential way-point manoeuvering of ships," in *Proc. 43rd IEEE Conference on Decision and Control*, vol. 5, Bahamas, December 2004, pp. 5360–5367.

[4] T. Fossen, M. Breivik, and R. Skjetne, "Line-of-sight path following of underactuated marine craft," in *Proc. 6th IFAC MCMC*, Girona, Spain, September 2003, pp. 244–249.

[5] M. Breivik and T. Fossen, "Path following of straight lines and circles for marine surface vessels," in *Proc. 6th IFAC CAMS*, Ancona, Italy, July 2004, pp. 65–70.

[6] P. Encarnação, A. Pascoal, and M. Arcak, "Path following for autonomous marine craft," in *Proc. of 5th IFAC Conference on Maneuvering and Control Marine Craft*, 2000, pp. 117–122.

[7] P. Encarnação and A. Pascoal, "3d path following for autonomous underwater vehicle," in *Proc. of 39th IEEE Conference on Decision and Control*, vol. 3, Sydney, Australia, December 2000, pp. 2977–2982.

[8] M. Aicardi, G. Casalino, G. Indiveri, A. Aguiar, P. Encarnação, and A. Pascoal, "A planar path following controller for underactuated marine vehicles," in *Proc. of 9th IEEE Mediterranean Conference on Control and Automation*, Dubrovnik, Croatia, June 2001.

[9] A. Aguiar and A. Pascoal, "Dynamic positioning and way-point tracking of underactuated auvs in the presence of ocean currents," in *Proc. of 41st IEEE Conference on Decision and Control*, vol. 2, Las Vegas NV, December 2002, pp. 2105–2110.

[10] A. Healey and D. Lienard, "Multivariable sliding-mode control for autonomous diving and steering of unmanned underwater vehicles," *IEEE Journal of Oceanic Engineering*, vol. 18, no. 3, pp. 327–339, July 1993.

[11] R. Brockett, "Asymptotic stability and feedback stabilization," *Differential Geometry Control Theory*, pp. 181–208, 1983.

[12] A. Astolfi, "On the stabilization of nonholonomic systems," in *Proc. of the 33rd IEEE Conference on Decision and Control*, vol. 4. Lake Buena Vista, FL, USA: IEEE, December 1994, pp. 3481–3486.

[13] I. Kolmanovsky and N. McClamroch, "Developments in nonholonomic control problems," *IEEE Control Systems Magazine*, vol. 15, no. 6, pp. 20–36, December 1995.

[14] Z. Jiang and H. Nijmeijer, "Tracking control of mobile robots: A case study in backstepping," *Automatica*, vol. 33, no. 7, pp. 1393–1399, July 1997.

[15] E. Panteley, E. Lefeber, A. Loria, and H. Nijmeijer, "Exponential tracking control of mobile car using a cascaded approach," in *Proceedings of the IFAC Workshop on Motion Control*, Grenoble, France, 1998, pp. 221–226.

[16] A. Aguiar, A. Atassi, and A. Pascoal, "Regulation of a nonholonomic dynamic wheeled mobile robot with parametric modeling uncertainty using lyapunov functions," in *Proc. of 39th IEEE Conference on Decision and Control*, vol. 3. Sydney, Australia: IEEE, December 2000, pp. 2995–3000.

[17] O. Sørdalen and O. Egeland, "Exponential stabilization of nonholonomic chained systems," *IEEE Trans. Automatic Control*, vol. 40, no. 1, pp. 35–49, January 1995.

[18] E. Lefeber, "Tracking control of nonlinear mechanical systems," Ph.D. dissertation, University of Twente, The Netherlands, 2000.

[19] H. Goldstein, *Classical Mechanics*, 2nd ed. Addison-Wesley, July 1980.

[20] H. Khalil, *Nonlinear Systems*, 3rd ed. Upper Saddle River, New Jersey, USA: Pearson Education International inc., 2000.

[21] V. Utkin, "Variable structure systems with sliding modes," *IEEE Trans. Automatic Control*, vol. AC-22, no. 2, pp. 212–222, April 1977.

[22] R. DeCarlo, S. Zak, and G. Mathews, "Variable structure control of of non-linear multivariable systems: A tutorial," in *Proc. IEEE*, vol. 76, March 1988, pp. 212–232.